A 2020 view of tension-based cortical morphogenesis

David C. Van Essen[a,1]

[a]Department of Neuroscience, Washington University School of Medicine, Saint Louis, MO 63110

This contribution is part of the special series of Inaugural Articles by members of the National Academy of Sciences elected in 2017.

Contributed by David C. Van Essen, October 24, 2020 (sent for review August 17, 2020; reviewed by Christopher D. Kroenke and Tomasz J. Nowakowski)

Mechanical tension along the length of axons, dendrites, and glial processes has been proposed as a major contributor to morphogenesis throughout the nervous system [D. C. Van Essen, *Nature* 385, 313–318 (1997)]. Tension-based morphogenesis (TBM) is a conceptually simple and general hypothesis based on physical forces that help shape all living things. Moreover, if each axon and dendrite strive to shorten while preserving connectivity, aggregate wiring length would remain low. TBM can explain key aspects of how the cerebral and cerebellar cortices remain thin, expand in surface area, and acquire their distinctive folds. This article reviews progress since 1997 relevant to TBM and other candidate morphogenetic mechanisms. At a cellular level, studies of diverse cell types in vitro and in vivo demonstrate that tension plays a major role in many developmental events. At a tissue level, I propose a differential expansion sandwich plus (DES+) revision to the original TBM model for cerebral cortical expansion and folding. It invokes tangential tension and "sulcal zipping" forces along the outer cortical margin as well as tension in the white matter core, together competing against radially biased tension in the cortical gray matter. Evidence for and against the DES+ model is discussed, and experiments are proposed to address key tenets of the DES+ model. For cerebellar cortex, a cerebellar multilayer sandwich (CMS) model is proposed that can account for many distinctive features, including its unique, accordion-like folding in the adult, and experiments are proposed to address its specific tenets.

cerebral cortex | cerebellum | folding | biomechanics | gyrification

Morphogenesis, the process whereby bodies and brains acquire their distinctive shapes, has fascinated scientists for centuries. Morphogenesis of the nervous system is particularly intriguing, given the sheer number of neural subdivisions, their intricate shapes, and the staggering complexity of local and long-distance wiring. The mammalian cerebral cortex has attracted special attention, as it is physically dominant and mediates a wide range of functions. The convolutions of human cerebral cortex are notable for their complexity, individual variability, and susceptibility to abnormal folding in many brain disorders. Cerebellar cortex has received less attention but is equally intriguing as to how it acquires its accordion-like parallel folds.

In 1997, I proposed that mechanical tension along the length of axons, dendrites, and glial processes contributes to many aspects of morphogenesis throughout the nervous system (1). Cerebral cortex was the premier examplar for this general tension-based morphogenesis (TBM) hypothesis. As originally formulated, radially biased tension along dendrites and axons within cortical gray matter (CGM) can explain why the cortex is a thin sheet that expands preferentially in the tangential domain. With increasing brain size, cerebral cortex increases disproportionately relative to subcortical domains (2). Consequently, beyond a critical surface area, tangential cortical expansion exceeds what is needed to envelop the underlying subcortical structures, and cortical folding ensues (3, 4). Axonal tension in the underlying core that includes white matter (WM) can explain why the cortex folds to bring strongly connected regions closer together and make WM compact. The TBM hypothesis is based on physical forces (tension and pressure) that must shape all living things (5). TBM would naturally reduce overall wiring length if all neuronal processes strive to reduce their length while preserving their connectivity, thereby benefitting processing speed and energy efficiency. Initial support for TBM included pioneering in vitro studies showing that neurites can generate tension, elongate when towed, and retract on release of tension (6–8).

Here, I review a burgeoning literature since 1997 that provides extensive evidence and arguments bearing on the TBM hypothesis. Studies at molecular and cellular levels have deepened our understanding of how mechanical tension works against osmotic pressure and focally directed pressure to maintain and modify cell shape. The workhorse "toolkit" for tissue morphogenesis is the intracellular cytoskeleton, an intricate network dominated by elongated macromolecular filaments whose length, bundling, and anchoring to the plasma membrane and to various organelles are regulated by a plethora of adjunct molecules.

At the tissue level, evidence both for and against the TBM cortical folding hypothesis has been reported. Here, I propose a "differential expansion sandwich plus" (DES+) model that preserves key aspects of the original TBM model but incorporates additional features that enhance its explanatory power. In brief, the DES+ model includes the following tenets: 1) Tangential cortical expansion is promoted by radially biased tension in CGM, supplemented by cerebrospinal fluid (CSF) pressure at early ages. 2) Differential tangential expansion along the cortex/core boundary promotes folding via two complementary mechanisms: 2A) Pathway-specific tension promotes gyral folds at specific locations and 2B) tethering tension promotes buckling along the cortex/core boundary. 3) Tangential tension in an outer

Significance

Brain structures change shape dramatically during development. Elucidating the mechanisms of morphogenesis provides insights relevant to understanding brain function in health and disease. The tension-based morphogenesis (TBM) hypothesis posits that mechanical tension along axons, dendrites, and glial processes contributes to many aspects of central nervous system morphogenesis. Since TBM was proposed in 1997, extensive evidence supports a role for tension in diverse cellular phenomena, but tension's role in cortical folding has been controversial. An extensively revised version of the TBM model for cerebral cortex addresses limitations of the original model, incorporates new features, and can be tested by many experimental approaches. For cerebellar cortex, a revised model accounts for many aspects of its development and adult architecture.

Author contributions: D.C.V.E. designed research, performed research, analyzed data, and wrote the paper.

Reviewers: C.D.K., Oregon Health & Science University; and T.J.N., University of California, San Francisco.

The author declares no competing interest.

[1]Email: vanessen@wustl.edu.

This article contains supporting information online at https://www.pnas.org/lookup/suppl/doi:10.1073/pnas.2016830117/-/DCSupplemental.

First published December 15, 2020.

cortical layer (the third layer of the DES+ "sandwich") combines with transsulcal adhesion of the leptomeninges (pia and arachnoid layers) to promote buckling, sulcal invagination, and "sulcal zippering." 4) Patterns of proliferation and migration impact early three-dimensional (3D) brain geometry, indirectly influence the location of cortical folds and the axis of folding, and constitute the "+" of the DES+ model. 5) Tension throughout the central nervous system (CNS) reduces wiring length and interstitial space, subject to the topological constraints imposed by axonal interdigitation.

A variety of approaches are proposed to test the first three tenets. With regard to cerebellar cortex, a different type of multilayer sandwich model is proposed that can account for many distinctive aspects of cerebellar morphogenesis and adult architecture. Before detailed consideration of the DES+ model, it is useful to 1) introduce a biomechanical perspective and framework, 2) summarize key evidence regarding how tension operates at a cellular level, and 3) review key developmental events during forebrain morphogenesis.

A Biomechanical Framework for CNS Morphogenesis

In his classic treatise *On Growth and Form*, D'Arcy Thompson (5) proposed that morphogenesis is largely driven by an interplay between mechanical tension and pressure acting on structures having physical asymmetries and anisotropies. Thompson (5) focused on nonneural biological structures, but these principles apply equally well to the nervous system. A starting point is to consider the types of material properties and physical forces involved.

Material Properties. Developing CNS tissue is soft and pliable (*SI Appendix*, Topic 1) and grows in an incompressible fluid environment. Except for the pia mater and arterial and venous linings, its extracellular matrix (ECM) largely lacks components such as collagen that stiffen peripheral tissues (9–12). Three types of biomechanical properties relevant to morphogenesis can be assayed in tissues, cells, or molecules by measuring physical deformation (strain) in response to applied force (stress) (13): 1) Elasticity (compliance) and its inverse, stiffness, reflect linear, time-independent deformation measured under linearly aligned stress (tensile and compressive stiffness) or more complex stress configurations (bending and shear stiffness). Purely elastic material returns to its original configuration after force removal. 2) Viscosity reflects fluid resistance to flow in response to applied pressure, manifested by a time-dependent displacement under constant force. 3) Plastic behavior involves nonelastic deformation without recovery after force release. Developing neurons and neural tissue commonly display viscoelastic and plastic behavior.

Forces. Five types of physical force are especially relevant to CNS morphogenesis: 1) Omnidirectional fluid pressure arising from macroscopic fluid production (e.g., intraventricular CSF) or from osmotic imbalance across a cell's plasma membrane spreads in all directions until reaching a diffusion barrier. 2) Surface tension and interfacial tension are tangential forces that strive to reduce the surface area of an interface between two materials. In biology, fluid pressure across an epithelium sealed by tight junctions causes macroscopic interfacial tension. Microscopic surface tension arises at the plasma membrane lipid/aqueous interface and is enhanced by interfacial tension from an underlying actin-rich cytoskeletal "cortex" (14). 3) Microscopic directed pressure can be highly anisotropic, but only when cellular components (e.g., bundled filaments) have high bending stiffness as they push. 4) Axial tension occurs when elongated cellular components actively generate a longitudinal shortening force or when elastic or viscoelastic components are passively stretched while anchored at both ends. 5) Adhesiveness reflects the tendency of a cellular constituent to stick to something else, including molecules in the ECM that surrounds CNS cells and has its own distinctive material properties (15), even when forces are trying to pull the components apart.

Tensegrity. A tensegrity structure, as promulgated by Buckminster Fuller (16) for architecture and by Donald Ingber (17, 18) for cell biology, attains stability by having some components under tension and others under compression, rather than the predominantly compressive forces that support conventional buildings. In a geodesic dome the distribution of struts under tension vs. compression depends on external forces (e.g., gravity and wind) and can change rapidly (e.g., in a storm). In cell biology, focal adhesions to external substrates can transfer tension and strongly influence cell geometry (19). Living cells are not floppy bags of molecular and macromolecular soup but rather "prestressed" tensegrity structures responsive to dynamic developmental and environmental forces.

Biomechanics of Tissue Expansion. Key aspects of tissue growth in developing CNS tissue can be considered in relation to a schematic 3D grid of small volume elements ("voxels" in Fig. 1). Tissue expansion in a given voxel is indicated by a tiny "growth bubble" whose size reflects the net change in volume per unit time (from expansion of existing cells and ingrowth of new cells, less any material loss; see also figures 1.5 and 12.1 in ref. 20). If tissue compliance is isotropic and there is no external pressure differential, expansion will also be isotropic, represented by a spherical growth bubble and equal-sized green expansion arrows (Fig. 1*A*). Anisotropic tissue compliance such as that caused by radially biased tension (Fig. 1*B*, red arrows) leads to anisotropic tissue expansion—an ellipsoidal growth bubble (of equal volume) and unequal green expansion arrows (Fig. 1*B*). Importantly, these tissue expansion patterns are independent of the direction of cellular migration or ingrowth. Thus, growing axons do not push tissue "ahead" to form a gyrus (as suggested in ref. 21), and migrating neurons do not push cells "to the side" (as suggested in ref. 22).

It is also important to consider asymmetric or anisotropic forces external to a given tissue compartment that can modify cellular architecture (see below). External forces that fold a thick viscoelastic slab generate compressive forces near the fold's interior crease, tensile (stretching) forces near its exterior margin, and shearing stresses throughout (23).

Cellular Forces and Mechanisms

Cytoskeletal and Related Components. Neuronal morphology in its magnificent diversity is established, maintained, and modified

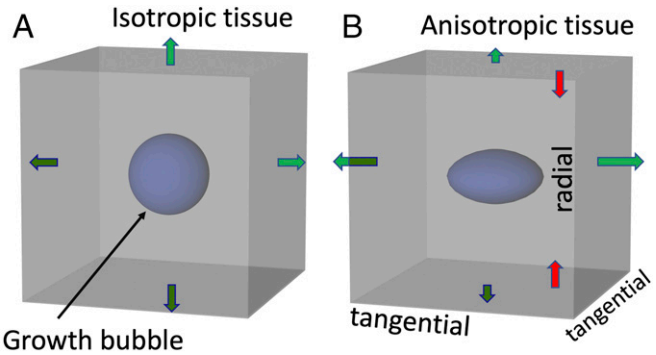

Fig. 1. (*A*) Spherical growth bubble and isotropic expansion (green arrows) in a cubical tissue "voxel" with isotropic compliance. (*B*) Oblate spheroidal growth bubble in a voxel with radially biased tension (red arrows) and hence anisotropic compliance and expansion.

mainly by the cytoskeleton. Fig. 2 schematizes how four cytoskeletal macromolecules play dominant roles in cellular force generation and transmission in seven common events during neural development. 1) Filamentous actin (F-actin) is a polarized filament whose length is dynamically regulated by polymerization of globular actin (G-actin) subunits at one end and depolymerization at the other. F-actin can be cross-linked into stiff bundles (e.g., in growth cone filopodia), an irregular mesh (in lamellopodia), or ring-like structures in axons (24–27). 2) Many myosin subtypes interact with F-actin to generate force via multiple mechanisms (14, 28–30). 3) Microtubules are tubular, larger in diameter than F-actin, lengthened via subunit assembly at one end, and shortened by disassembly at the other (31). They can be cross-linked into stiff bundles (32), and sliding between microtubules can generate a pushing force mediated by molecular motors (28, 33). 4) Anchoring molecules, particularly transmembrane integrins, mediate focal adhesion to the plasma membrane (26, 34, 35) by anchoring F-actin, microtubules, and other filaments internally and binding externally to the ECM, a network of proteins, proteoglycans, and other molecules that occupy interstitial space and also constitute the basal lamina (basement membrane) at the pial surface (36). Another subsystem regulates osmotic pressure across the plasma membrane by transmembrane transport of ions, water, and other constituents (37).

Growth Cones. Growth cones enable axons, dendrites, and migrating cells to advance, retract, or turn based on local chemical and mechanical cues. Actin polymerization in lamellopodia and filopodia can push the plasma membrane forward by directed pressure (red arrows, event 1 in Fig. 2) (27, 38). Adhesion of the growth cone tip to ECM molecules (event 2) enables actomyosin-mediated traction to advance the growth cone (39, 40) and transfer tension to the growth cone rear (event 3) (27).

Axons and Neurites. "Neurites" (not explicitly classified as axons or dendrites) studied in vitro commonly exhibit three key characteristics: resting tension, retraction on tension release, and elongation when pulled ("towed growth"). Resting tension has been demonstrated in vitro for many neuronal types and species and in vivo for invertebrate axons (41–43). Tension magnitude varies widely (13), but should suffice to drive morphogenesis in highly compliant neural tissue (*SI Appendix*, Topic 1). Axons can transfer tension from the growth cone (event 3 in Fig. 2) and also generate tension along their length (event 4 in Fig. 2) by an actomyosin-based process likely involving circumferential F-actin rings (6, 24, 44). When tension is relaxed, retraction commonly occurs (45). Towed growth can increase axonal length dramatically while maintaining diameter (46, 47), likely involving pushing from microtubule sliding (event 5 in Fig. 2) (48, 49).

Glial and Dendritic Processes. Evidence for resting tension in glial cell processes comes from tissue cuts in developing cerebellum (50) and viscoelasticity observations in retina (51). Resting tension in dendrites has been challenging to demonstrate directly but is consistent with dendritic elongation via growth cones (52), the presence of dendritic actin–spectrin rings (53) akin to those implicated in axonal tension, plus indirect evidence discussed below.

Migration and Cytokinesis. Neurons often migrate considerable distances from birthplace to destination (54). In radial migration, a leading process growth cone crawls along an anchored radial glial scaffold and passively pulls the centrosome via microtubule assemblies (event 6 in Fig. 2); the nucleus may be pulled passively via microtubules (event 7) or pushed by myosin-based squeezing (54). Tangentially migrating neurons lack a glial scaffold, but their leading processes (54) may advance by latching onto the ECM of vascular endothelial cells (55). During cytokinesis of glial and neural progenitors, nuclear translocation can occur along processes anchored to the ventricular (apical) and/or pial (basal) surfaces (56), likely involving microtubule-mediated pulling of the centrosome and nucleus (events 6 and 7 in Fig. 2) (57–59).

Early Forebrain Development

Tissue Growth and Mechanics. The embryonic mammalian forebrain gives rise to cerebral cortex plus many subcortical nuclei via an intricately choreographed process involving multiple proliferative zones and other transient structures. This section emphasizes key events in human and macaque forebrain development but also draws on findings in ferret and mouse.

Forebrain Vesicles and Ventricles. The telencephalic and diencephalic vesicles arise and become inflated by virtue of 1) rapid neuroepithelial cell proliferation in the anterior neural tube, 2) sealing of the anterior neuropore to impede CSF efflux, 3) actomyosin-based constrictions that separate embryonic vesicles (60), and 4) a pressure differential across the tight-junction–coupled neuroepithelium driven by ion pumps and

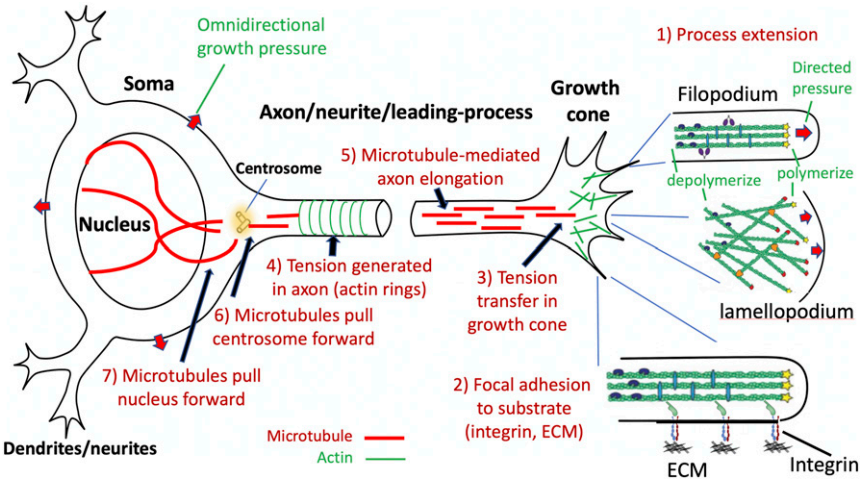

Fig. 2. Key events and cellular components in a prototypical developing neuron during axonal/neurite outgrowth and cell migration. These events may occur concurrently or in any sequence.

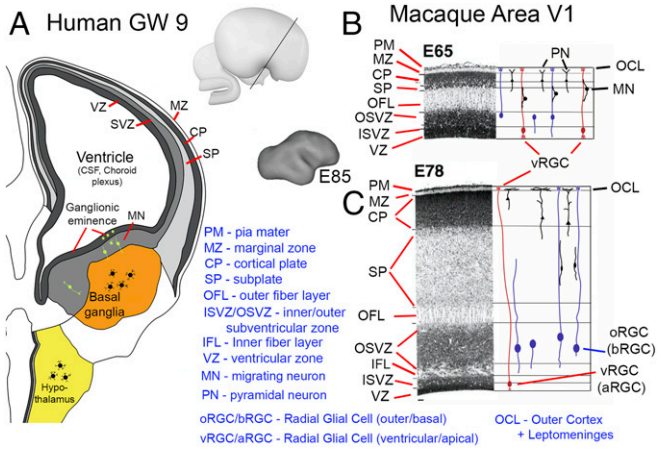

Fig. 3. Primate forebrain development. (*A*) Schematic of human coronal section at GW9. Copyright (2006) from ref. 63. Reproduced by permission of Taylor and Francis Group, LLC, a division of Informa plc. (*B* and *C*) Nissl-stained sections from macaque cortical area V1 at embryonic days E65 and E78, respectively, with schematics of glial and neuronal morphologies. Reprinted from ref. 65, by permission of Oxford University Press.

protein and proteoglycan secretion (37) (*SI Appendix*, Topic 1). The choroid plexus emerges as a vascularized structure whose epithelial layer produces CSF (61) plus growth factors that promote neuroepithelial proliferation (62), and the forebrain vesicles differentiate into ventricles proper. In humans, the lateral ventricles expand rapidly along with the thin cortical sheet (Fig. 3*A*).

Subcortical Nuclei. Forebrain subcortical nuclei arise from the ventricular germinal zone of the diencephalon and ventromedial telencephalon (63). Postmitotic diencephalic neurons migrate mainly laterally and settle in nearby target regions that become specific thalamic and hypothalamic nuclei, each generally compact but irregularly shaped (yellow in Fig. 3*A*). The diencephalic vesicle collapses into the narrow third ventricle lined by a thick gray matter wall. In the telencephalon, the blob-like ganglionic eminence bulges into the lateral ventricle. Many postmitotic neurons from the ganglionic eminence migrate ventrally and coalesce to form the basal ganglia nearby (orange in Fig. 3*A*).

Tension Explains Quasi-Isotropic Subcortical Expansion. Neurons in forebrain subcortical nuclei typically develop multipolar, irregularly oriented dendrites (64) intertwined with one another and with highly branched intrinsic and afferent axons. If these dendrites and local axons are under tension, their quasi-isotropic morphology should result in quasi-isotropic subcortical tissue compliance and tissue expansion (as in Fig. 1*A*), thereby accounting for their mostly blob-like adult shapes (1). Alternative morphogenetic mechanisms have not to my knowledge been proposed for the shapes of typical subcortical nuclei. *SI Appendix*, Topic 2 addresses an outlier case, explaining why the tail of the caudate nucleus in primates has a uniquely elongated shape and an associated architectural anisotropy discernible using diffusion MRI.

An Extended Proliferative Period for Cerebral Cortex Neurons. Cerebral cortical neurons greatly outnumber subcortical neurons, especially in gyrencephalic species, as a consequence of several developmental factors: 1) The balloon-like ventricular expansion (Fig. 3*A*) preferentially increases the surface area of the cortical portion of the proliferative ventricular zone. 2) Cortical germinal layers add inner subventricular zones (ISVZ) and outer subventricular zones (OSVZ), increasing the proliferative pool (65). 3) A prolonged neuronal proliferation period (red bars in Fig. 4 *A* and *B*) allows many rounds of mitosis. In macaque area V1, neurons are born during the 2 mo between approximately embryonic day 45 (~E45) and ~E102 (66, 67). Neuronal proliferation for human cortex is even longer, extending from approximately gestation week 6 (~GW6) into the third trimester (68). As proliferation subsides, the ventricular zone becomes an ependymal cell layer (69) no longer sealed by tight junctions (70, 71), thus facilitating CSF seepage through the brain parenchyma. *SI Appendix*, Topic 3 discusses why, from evolutionary and computational perspectives, cerebral cortex remains thin but expands disproportionately with brain size.

Radial and Tangential Migration. Postmitotic excitatory neurons born in the ventricular zone migrate radially along a scaffold of ventricular radial glial cells (vRGC) (a.k.a. apical RGC [aRGC]) anchored at ventricular and pial surfaces. In primates, neuronal proliferation in the subventricular zones, especially the OSVZ, continues beyond that of vRGCs (68) and involves multiple outer radial glial cell subtypes (oRGC) (a.k.a. basal RGC [bRGC]) whose processes extend apically and/or basally (Fig. 3*C*) (56, 72–74). Later-born neurons migrate mostly along radially oriented oRGC basal processes, many of which are likely anchored within the OSVZ as well as at the pial surface and are under tension as the cerebral wall expands (72, 75). Neurons reaching the cortical plate migrate past deeper (earlier-born) cortical neurons and settle superficially, just below the marginal zone (MZ) that contains early-arriving Cajal–Retzius cells and later becomes layer 1 (76, 77). Migration (orange bars in Fig. 4 *A* and *B*) extends well beyond the neural proliferation period.

Excitatory pyramidal cells extend a descending axon plus an apical dendrite, typically with an apical tuft in the MZ (25, 65, 76). As additional migrating neurons settle more superficially in the cortical plate, the apical dendrites of deeper-layer pyramidal cells remain anchored in the MZ and presumably lengthen by towed growth akin to that observed in vitro (Fig. 3*C*) (77, 78). Inhibitory interneurons migrate tangentially from the ganglionic eminence (54). In the macaque, glial cells arise mainly from the OSVZ as neuronal proliferation winds down (79).

The Outer Cortex + Leptomeningeal Layer. The outer (basal) cortical surface is bounded by the pia mater, which includes a thin

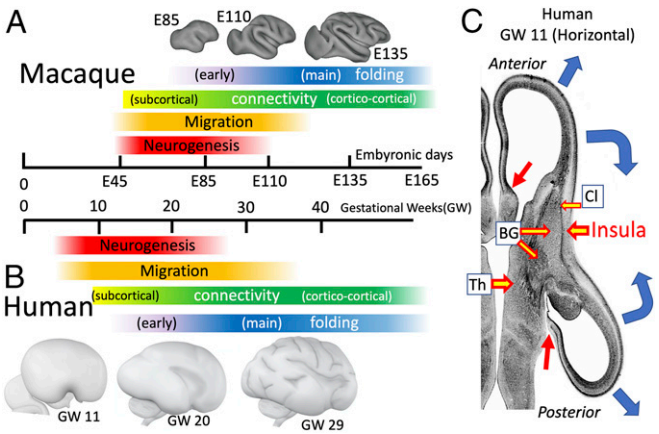

Fig. 4. (*A* and *B*) Timing of major events in macaque (*A*) and human (*B*) cortical development. (*C*) Location of future insular cortex relative to claustrum (Cl), basal ganglia (BG), thalamus (Th), and lateral ventricles in human at GW11. Blue arrows, cortical expansion trajectories; red arrows, junction between neocortex and subcortical medial wall. (*A*) Macaque surface models are reprinted from ref. 106, which is licensed under CC BY 4.0. (*C*) Republished with permission of Taylor & Francis Group LLC – Books, from ref. 63; permission conveyed through Copyright Clearance Center, Inc.

layer of pial cells; an acellular and stiff basal lamina containing collagen, laminins, etc. (80); an ECM that may extend into the arachnoid layer; and a vasculature that early on contains a plexus of pial capillaries (81). The MZ (later layer 1), pia mater, and adjacent arachnoid layers are anatomically distinct, but are considered here as an outer cortical + leptomeningeal (OCL) zone/layer (Fig. 3*B*) that works in concert to generate tangential morphogenetic forces.

Cortical Subplate and Fiber-Rich Zones. The cortical subplate (SP) (Fig. 3), between the cortical plate and the outer fiber layer (OFL), is a transient but at times thick layer (63, 65, 82, 83). It is fiber rich but contains migrating neurons plus a sparse but persistent population of morphologically heterogeneous neurons (84, 85), and it serves as a transient waiting zone for thalamocortical and and cortico-cortical projections (86, 87) (but see ref. 88). The initially thin OFL thickens and transitions to WM along with the subplate and OSVZ. The subcortical WM core and its precursors are considered a single layer in the current framing of the DES+ model despite its multilaminated fibrillar and cellular strata (63, 82, 89).

Connectivity and Gyrification. In humans, early-forming long-distance fiber pathways involving cerebral cortex (Fig. 4*B*, yellow portion of connectivity bar) include the internal capsule (starting ~GW8) and corpus callosum (starting ~GW13.5) (82). Cortical synapse formation and WM expansion involving cortico-cortical and cortico-subcortical pathways occur throughout the third trimester (68) (green portion of connectivity bar) and match the main period of gyrification (blue portion of folding bar) (82). In the macaque (Fig. 4*A*), long-distance cortico-cortical connections reach the subplate and/or cortical plate beginning ~E106 for area V4 (87) and ~E108 for V1-V2 (90). This overlaps with the main gyrification period (~E100 to ~E135) (91–93). Axons tend to run in parallel in the developing white matter, forming numerous long-distance fiber tracts. However, extensive crossing of fiber bundles must occur to achieve the brain's enormous wiring complexity (e.g., an average of >50 input and output pathways to each cortical area in the macaque) (94). Hence, white matter wiring must have high topological complexity, which has important implications for aggregate wiring length as the brain grows (see below).

Three-Dimensional Landscape Prior to Gyrification. The insula and Sylvian fissure profoundly impact overall cerebral shape in primates. Insular cortex arises early from a specialized germinal region (95) and is anchored by its connections with the adjacent slow-growing claustrum and basal ganglia (Fig. 4*C*). Neighboring neocortex expands rapidly (blue arrows), surrounding the insula by GW20 and forming a complete Sylvian fissure by GW29 (Fig. 4 *B*, *Bottom* row). Near the midline the cortical sheet merges with subcortical structures (red arrows in Fig. 4*C*); the noncortical "medial wall" occupies the gap. At GW20, the 3D landscape is generally smooth but curved to varying degrees: rounded like a ball near occipital and frontal poles, quasi-cylindrical in some temporal and peri-Sylvian regions, and saddle shaped in a few locations. These 3D features may bias the axis of cortical folding (see below and ref. 96).

Early Cortical Folds. An important but understudied early phase of cortical folding occurs in primates (purple portion of folding bars in Fig. 4). Most strikingly, the calcarine sulcus (CaS) appears by GW13.5 in humans (82) (Fig. 5 *A* and *B*) and by E85 in macaques (91). The associated cerebral wall is notably thin (red arrows) except for the marginal zone (green arrows) and protrudes deeply into the ventricle.

Also appearing early in the second trimester in humans are small dimples and wrinkles (Fig. 5 *C* and *D*) that are irregular in location and spacing and might only be transient (82). Importantly, invaginations are typically most pronounced in superficial layers, suggesting they are initiated by superficial morphogenetic forces. Remarkably, addition of several ECM components to human organotypic neocortical slice cultures induces invaginations that are most pronounced in superficial layers and include basal lamina "fingers" extending into each invagination (97) (*SI Appendix*, Topic 4). These observations help motivate the proposed role of the OCL in the DES+ model.

Key Folding and Thickness Characteristics. Models of cortical expansion and folding should aim to account for many observations, including the following: 1) Folding and folding-function consistencies: In moderately gyrencephalic species, cortical folding is consistent across individuals and is closely correlated with areal boundaries (folding-function consistency), as demonstrated most clearly in the macaque (1, 98, 99). 2) Folding and folding-function variability: In contrast, human cortex shows much greater individual variability in folding and folding-function correlations, although regularities persist for primary folds (99–101). 3) Folding-related architectonic distortions: Cortical folding is associated with systematic distortions of laminar and radial organization and cellular morphology (75, 102, 103). In gyral crowns, radial axes diverge from the base; deeper layers are thicker and have tall, narrow dendritic arbors vs. short, wide arbors in thinner superficial layers. In sulcal fundi, the pattern is reversed. 4) Cross-sulcal adherence: In countless published human structural MRI images and in gently processed histological sections from healthy adult brains, apposed banks of sulci generally are contiguous with one another along the pia mater over extended regions, except where blood vessels intervene (*SI Appendix*, Topic 2 and Fig. S1). This adherence may be mediated by a thin intervening ECM layer, as occurs in other tissues, where apposed basal laminae may adhere to or slide past

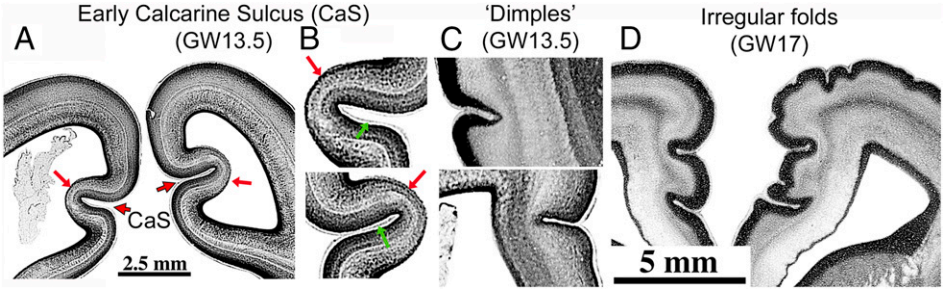

Fig. 5. Early-forming cortical sulci in humans. (*A* and *B*) Calcarine sulcus at GW13.5 (coronal). (*C*) "Dimples" in lateral temporal (*Top*) and medial frontal (*Bottom*) GW13.5 cortex. (*D*) Early irregular folds in frontal cortex at GW17. Republished with permission of Taylor & Francis Group LLC – Books, from ref. 82; permission conveyed through Copyright Clearance Center, Inc.

one another (104). 5) Cortical thickness: Cortex tends to be thinner in sulcal fundi and thicker in gyral crowns (75). Also, each cortical area has a characteristic thickness, which in adult humans varies approximetaly twofold across cortical areas (105). 6) Folding abnormalities: Folding abnormalities occur in many human brain disorders (e.g., lissencephaly, polymicrogyria) and should be explicable in terms of altered folding mechanisms (*SI Appendix*, Topic 5).

Models and Mechanisms of Cerebral Cortical Expansion and Folding

Many candidate cortical folding models have been proposed over the past two centuries (75, 101, 106). As with many other developmental processes, multiple mechanisms are likely involved, especially given the complexity of events summarized in preceding sections. In recent years much attention has focused on various differential tangential expansion (DTE) models. The essential notion is that when adjacent layers expand at different rates, instabilities and/or biased forces along their common interface promote cortical folding. My original TBM hypothesis (1, 3) is in essence a bilayer tension DTE model that invokes differential expansion of cortex vs. the underlying WM-dominated core. The DES+ model proposed here additionally invokes tangential tension in the outermost OCL zone plus effects of 3D brain shape at the onset of folding. This section describes the DES+ model, evaluates evidence for and against it, illustrates complementarity between it and a recent computational simulation of a physical "gel-brain" model, and proposes experimental approaches to address key unresolved mechanistic issues.

The DES+ Model. Fig. 6 schematizes major morphogenetic forces proposed for each layer. The model's core tenets represent mechanistically distinct components that can operate in concert and presumably contribute to different degrees according to region and developmental stage.

Tenet 1. Radially biased tension promotes tangential cortical expansion and is supplemented by CSF pressure at early ages. Initially, tension along radial processes of neuroepithelial and radial glial cells combines with elevated CSF pressure to expand the nascent cerebral wall and keep it thin, akin to inflating a balloon. Once migrating neurons establish the cortical plate, tension along pyramidal cell apical dendrites anchored by apical tufts in the MZ and by cell bodies and basal dendrites in deeper layers (red arrows) make CGM stiffer along radial vs. tangential axes (pink elliptical growth bubbles) (cf. Fig. 1), thus promoting tangential expansion.

Tenet 2. Differential tangential expansion along the cortex/core boundary promotes folding. Except for the medial wall gap (Fig. 4*C*), cerebral cortex surrounds a subcortical core that includes WM, ventricles, and forebrain subcortical nuclei in adults, plus subplate, fibrous, and proliferative zones at earlier stages. The pattern of subcortical core expansion should reflect integrated growth across the volume, schematized by the magnitude and orientation of local growth bubbles. Cortex remains smooth if the expanding exterior of this core matches tangential cortical expansion, as occurs early in development in all mammals and into adulthood in lissencephalic species. In gyrencephalic species, instabilities arise along the cortex/core boundary once cortical surface area expands beyond that needed to enshroud a smooth core. Tension along axons and glia that cross this boundary prevents overt separation between the CGM and core. Instead, the exterior of the subcortical core must expand by folding to match that of the adjacent cortical sheet. This can be manifested in two distinct ways in terms of the location and pattern of folding.

Tenet 2A. Pathway-specific tension promotes gyral folds. Pathway-specific tension along axons interconnecting nearby cortical areas tends to bring strongly connected regions close together, forming a gyrus in between. Importantly, interareal connections tend to be strongest between nearby areas, and on average connectivity declines exponentially with distance (via WM) between areas (107). Given this distributional bias, pathways linking nearby areas should strongly influence folding patterns unless these pathways selectively lack tension (see below).

Tenet 2B. Tethering tension promotes buckling along the cortex/core boundary. Axons and radial glial processes whose trajectories include a strong component oriented

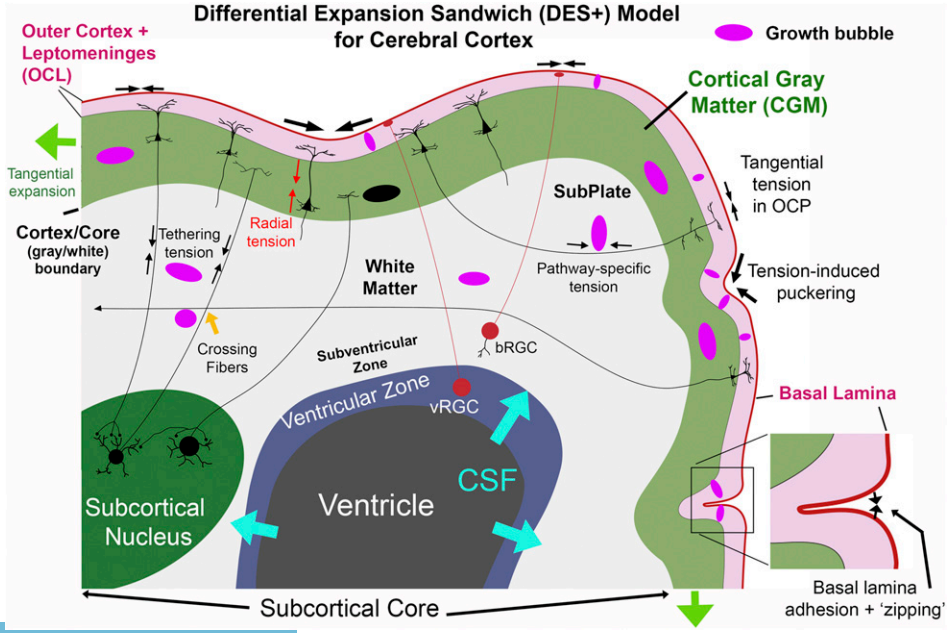

Fig. 6. Schematic of the DES+ model for cerebral cortex. See main text for explanation.

toward deeper parts of the subcortical core generate tethering tension that anchors the cortical sheet to the interior and promotes buckling once instabilities arise along the cortex/core boundary, rather than allowing fluid-filled "blisters" to form along the boundary. The distinction between tethering and pathway-specific tension is not an all-or-nothing dichotomy; many axons likely contribute to both processes.

Tenet 3. Tangential tension in the OCL layer and transsulcal pial adhesion promote buckling and sulcal invagination. Candidate sources of tangential tension in the OCL layer include 1) obliquely and tangentially oriented apical tufts of pyramidal cell apical dendrites; 2) tangentially oriented axons from extrinsic and intrinsic cortical neurons; 3) axons and dendrites of Cajal–Retzius cells; and 4) passive stretching of the acellular, stiff basal lamina induced by CGM expansion. In addition, adhesion between pial surfaces on opposing sulcal banks may promote sulcal "zipping."

OCL tension may account for cortical dimples occurring early in normal development (Fig. 5 *C* and *D*) and after experimental induction (97). As schematized on the right in Fig. 6, instabilities may arise when a local invagination ("puckering") alters local forces and/or material properties to promote further invagination (e.g., by inducing a nonlinear increase in OCL tension). When invagination brings the basal lamina on opposite sides of a crease into contact, adherence between opposing pial surfaces (via adhesive ECM intermediates) (*SI Appendix*, Topic 4) may stabilize the crease and also tend to "zip up" the interface and thereby deepen the invagination (Fig. 6, *Inset*). Other factors such as increased cortical plate compliance at the fundus of nascent sulci (97) might further promote invagination.

For the human CaS (Fig. 5 *A* and *B*) tensile and adhesive forces in the thick OCL might interact with mechanical properties of the much thinner subjacent layers of the cerebral wall to promote early and deep sulcal invagination into the ventricle. This distinctive internal bulge persists in adults as the calcar avis of the lateral ventricle (108).

Tenet 4. Three-dimensional geometry biases the location of folds and the axis of folding. The main period of gyrogenesis begins on a relatively smooth but complex 3D landscape generated by differential proliferation, migration, and differentiation (Fig. 4). In regions of locally elevated proliferation and migration the subcortical core will tend to bulge outward, as will the overlying CGM with its elevated number of neurons, setting up a bias for a gyral fold (109, 110). Regions that are curved in a quasi-cylindrical way (vs. flat, quasi-spherical, or saddle shaped), may be biased to fold along their long axis (96), as occurs most prominently in the temporal lobe (Figs. 4*B* and 7).

Tenet 5. Tension reduces wiring length and interstitial space. Resting tension along dendrites, axons, and glial processes should cooperatively make white and gray matter compact: 1) Axonal and dendritic tension takes up available slack and reduces wiring length throughout. 2) Brain growth is accommodated by tension-induced elongation that protects against axonal breakage. Importantly, wiring-length reduction must respect topological constraints imposed by crossing fiber bundles established prior to gyrification (*SI Appendix*, Topic 6). 3) Tension along all processes squeezes excess interstitial fluid out of CNS tissue (as in a sponge under pressure), with the pial basal lamina acting as a "shrink-wrapping" outermost layer. This prevents fluid accumulation from steady seepage of CSF through the brain parenchyma driven by ventricular CSF production (blue arrows in Fig. 6).

Correlative Evidence Supporting the DES+ Model. The DES+ model qualitatively accounts for several previously noted characteristics of cortical folding: 1) Folding-vs.-function consistencies can be explained by pathway-specific axonal folding forces that bias the location of gyral folds. In the macaque, gyri typically lie between nearby strongly connected areas (e.g., areas V1 and V2) (1, 98). However, detailed quantitative analyses have not been reported for any species. 2) Folding and folding-vs.-function variability in humans may reflect multiple factors. Individual differences in cortical area size (105) and connectivity (*SI Appendix*, Topic 7) may result in pathway-specific folding that varies across individuals. Greater tethering tension in the core and/or tangential tension in the OCL may increase buckling or quasi-random invaginations and thus folding-vs.-function variability. 3) Folding-related architectonic distortions: The aforementioned gyral vs. sulcal differences in laminar thickness and dendritic profiles qualitatively match the predicted internal strain patterns when external forces cause a slab to fold; the differences in cell morphology likely reflect dendritic lengthening via towed growth when stretched (tangentially or radially) and shortening by retraction when compressed. 4) Cortical thickness increases markedly during development (65) (Fig. 3 *B* and *C*) and correlates with a progressive decline in an initially high radial anisotropy (92). However, the tendency for cortex to be consistently thicker in gyral crowns and thinner in sulcal fundi (75) may involve a different mechanism (111).

Evidence for and against the Model from In Vitro Tissue Cuts. Tissue cuts made in brain slices of adult mice (112) and developing and adult ferrets (113) provide direct tests for tension in different brain locations. Cuts in deep cerebral white matter caused gaps indicative of resting tension in long-distance axons that presumably mediate tethering. Radial cuts in ferret cortex caused a gap in superficial but not deep layers, consistent with tangential tension in the OCL layer. However, counter to the DES+ model, tangential cuts in ferret CGM (113) failed to reveal resting radial tension. In white matter blades separating gyral folds, gaps occurred for cuts orthogonal but not parallel to the blade, suggesting that pathway-specific tension was selectively lacking in short-pathway cortico-cortical axons between opposing gyral banks. A critical issue is whether these ex vivo observations apply to developing cortex in vivo. This need not be the case, because tension ex vivo may have been partially obscured by tissue edema in and near metabolically active gray matter, stemming from osmotic shock and other side effects of slice preparation. Indeed, glutamate receptor activation and oxidative stress cause edema in brain slices (114, 115), strengthening the plausibility of this confound.

The apparent lack of radial tension within CGM and lack of axonal tension across gyral blades are both puzzling because, as discussed below, no biologically plausible alternative mechanisms have been proposed for preferential tangential expansion or for consistent gyral folding between strongly connected nearby cortical areas. Experiments to resolve these issues are proposed below.

A Complementary Gel-Brain Bilayer DTE Model. A striking physical and computational two-layer DTE model is based on a gel brain with an elastomer inner core shaped like an early (GW22) human fetal brain coated with a thin, softer outer layer (96). Immersion in a solvent (and running a matched computer simulation) caused the thin outer layer to expand faster, resulting in folding that broadly mimicked human cortical folding (Fig. 7). Importantly, the gel-brain and the DES+ models are strongly complementary. The gel-brain model explains the orientation of major folds as reflecting a smooth linear instability combined with a nonlinear sulcification instability operating on mechanical stress fields arising from the initial 3D brain shape (96). These

folding biases are consistent with DES+ tenet 4 but are not predicted by it in detail. On the flip side, the DES+ model explains five major phenomena not explicitly addressed by the gel-brain model but compatible with its framework: 1) Correlations between folds and areal boundaries and how these differ across species are explained by pathway-specific tension pitted against tethering tension and OCL tension (tenets 2 and 3). 2) Regulation of cortical thickness was constrained in the simulation to increase parametrically over time. Tenet 1 acccounts for thickness changes based on temporal and spatial patterns of radially biased tension. 3) Cohesion at the cortex/core boundary is achieved in the simulation by assumed physical continuity and in tenet 2 by tension along processes crossing this boundary. 4) Tangential cortical expansion exceeding growth of the subcortical core is achieved in the simulation by explicit growth equations and in tenets 1 and 5 by preferential tangential expansion of the CGM and compact wiring of the subcortical core. 5) Early cortical folds and dimples, neither reported nor excluded by the gel-brain simulation, are explained by tension fluctuations along the OCL layer and adhesiveness of the pial complex (tenet 3). Thus, a hybrid approach that incorporates the strengths of both the DES+ and gel-brain simulation models offers a promising avenue of exploration.

Comments on Other Models. Two other models of cortical expansion and folding do not explicitly invoke tension but, like the gel-brain simulation, are compatible with the DES+ model and appear to need tension to attain a biologically plausible instantiation. One is the radial intercalation model (22) for preferential tangential expansion. Another is a model of differential proliferation underneath gyral vs. sulcal regions leading to tangential dispersion of neurons in presumptive gyral regions as explanations for both preferential tangential expansion and cortical folding (110, 116, 117). *SI Appendix*, Topic 8 explains how these models can both be subsumed by tenet 1, argues that tangential dispersion is a consequence rather than a cause of tangential expansion, and critically evaluates a superficial-vs.-deep layer model of cortical buckling (118) and a "free energy" model of cortical folding (4).

Proposed Tests of the DES+ Model. The seven approaches outlined below highlight promising ways to address key open questions pertaining to the DES+ model: 1) Photoablation of cellular processes: A potentially powerful approach would be to focally photoablate individual fluorescently labeled dendrites, axons, and/or glial processes in mammals, as has been done in invertebrate axons (119), and then test for resting tension in different regions (CGM, OCL, gyral WM blades), orientations (radial vs. tangential), species, developmental ages, and in vivo (likely feasible in mice and ferrets) or in brain slices that are protected from edema (likely necessary for macaque studies). The magnitude and rate at which cut ends of a photoablated process retract may correlate with tension magnitude and might reveal any radial vs. tangential biases at each location. 2) Gyrification in mouse mutants and in vitro: Model systems for mechanistic studies of cortical gyrification include mutant mice (120, 121), human cerebral slice cultures (97), and stem-cell–derived cerebral organoids (122, 123). In such models it is important to distinguish between "bona fide" folding (with a smooth underlying ventricular suface) and wrinkling that includes all layers of the cerebral wall (75, 109) (*SI Appendix*, Topic 9). 3) Pial complex adhesion: In vitro experiments (e.g., using organotypic slice culture and free-floating tissue culture (97)) may enable analyses of the molecular basis of adhesion between apposed pial surfaces in nascent cortical sulci. Perturbation experiments akin to those in other model systems (104) may reveal effects of pial adhesions on other aspects of folding (*SI Appendix*, Topic 4). 4) Computational modeling: Aspects of cortical folding have been modeled using a variety of computational approaches. An attractive option involves computational simulations that incorporate neurobiologically realistic constraints. For example, a finite-element approach akin to that used for the gel-brain DTE model (96) might be adapted to incorporate biologically plausible pressure and tension as predicted by the DES+ model. 5) Biomechanical measurements of tissue properties: Recent methods such as magnetic resonance elastography (MRE) combined with focused ultrasound (FUS) might in principle test for the anisotropic compliance predicted by the DES+ model in white matter, and even CGM if sufficiently high spatial resolution can be achieved (*SI Appendix*, Topic 10). 6) Folding abnormalities in human brain disorders: Cortical folding abnormalities are profound in some disorders (e.g., lissencephaly) but modest or subtle in others such as Williams syndrome (124) and autism (125). Diverse mechanisms are likely involved in different disorders, including some that can be plausibly explained in terms of specific tenets of the DES+ model (*SI Appendix*, Topic 5). However, elucidation of disease mechanisms at cellular, molecular, and genetic as well as biomechanical levels will surely remain a major challenge for each disorder. 7) Possible roles of the vasculature in formation and/or stabilization of cortical folds should be explored, given that blood vessels undergo extensive modifications during gyrogenesis (126), including larger vessels embedded in the arachnoid that extend branches into apposed sulcal banks.

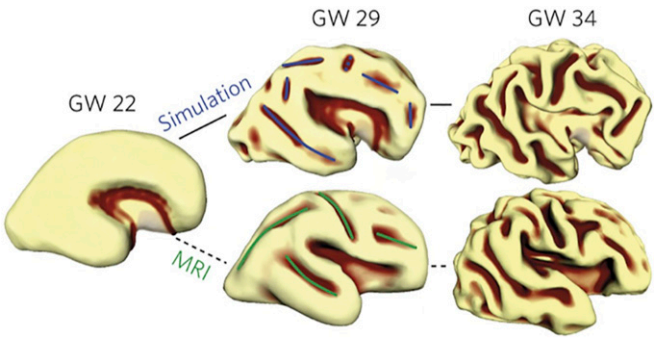

Fig. 7. Observed and simulated patterns of cortical folding. Starting from the 3D shape of a GW22 human fetal brain, the gel-brain simulation (*Top* row) and observed anatomical folding pattern (*Bottom* row) show striking similarities. Reprinted by permission from ref. 96 Springer Nature: Nature Physics, copyright 2016.

A Multilayer Model of Cerebellar Cortical Morphogenesis

Cerebellar Cortical Organization and Development. Cerebellar cortex is thin (approximately one-third of cerebral cortical thickness), comparable to one cerebral hemisphere in surface area, and tightly folded like an accordion (127). The mammalian cerebellum has 5 cardinal lobes (separated by 4 fissures), 10 lobules, and many finer-grained lamellae and folia in large-brain species (128, 129). Key features of adult cerebellar architecture (Fig. 8*A*) include a thin layer of Purkinje cells (PCs, red) and Bergmann radial glial cells (BGCs, green) above a dense layer of granule cells (GCs, blue) that have stubby, quasi-isotropic dendrites (128). GC axons ascend to the molecular layer (ML) and bifurcate into parallel fibers that synapse onto trellis-like PC ascending dendritic arbors. The thin cerebellar white matter contains three main axonal types: ascending mossy fibers (from the pons and other subcortical structures onto GCs), climbing fibers (from the inferior olive onto PCs), and Purkinje cell axons projecting to cerebellar nuclei (128, 130). Direct cerebellar cortico-cortical connections via white matter have not been reported. As with cerebral cortex, pial surfaces on apposed cerebellar folds typically abut one another directly (Fig. 8*C*) and appear to be adherent (*SI Appendix*, Topic 4 and Fig. S4). Finally, the granule cell layer (GCL) is thicker in gyral crowns and thinner

in sulcal fundi, whereas the ML is thicker in sulci than in gyri, similar to the pattern for layer 1 vs. deep layers of neocortex.

Cerebellar cortical development differs dramatically from that of cerebral cortex, although there are also important similarities. The earliest cerebellar neurons migrate from the rhombic lip anteriorly and then ventrally to form the cerebellar nuclei (131). The massively proliferating granule cell precursors (GCPs, blue) in the external germinal layer (EGL) also originate from the rhombic lip (132) (Fig. 8*B*). Above the EGL are the pia mater with basal lamina plus an arachnoid layer that (in contrast to cerebral cortex) is notably thick in humans and extends deep into cerebellar folds (133). PCs originate in the ventricular zone, migrate along radial glial cells (RGCs, purple) past the cerebellar nuclei (131) and settle below the EGL. Many RGCs lose their connection with the ventricular surface, migrate to the PC layer, and extend multiple processes to the pial surface (134) to become BGCs that are analogous to bRGCs in cerebral cortex (131, 135). Within the mouse EGL, GCPs have short leading and trailing processes and take divergent movement trajectories (50) as in a "can of worms." Postmitotic GCs extend processes medially and laterally, becoming parallel fibers that elongate within a rapidly thickening ML below the EGL. GCs migrate down BGC processes (with the GC ascending axons trailing behind) past the PC layer and settle in the inner granular layer (IGL) that becomes the GCL. In mice, major folds are initiated by "anchoring centers" (ACs) that are associated with 1) clustering and elongation of postmitotic GCs in the EGL, 2) maturation and invagination of PCs, and 3) convergence of BGC processes (136) (Fig. 8*B*). As the cortex expands tangentially, ACs remain anchored at the base of fissures and major folds (asterisks in Fig. 8*C*).

Mechanisms and Models of Cerebellar Development. Important mechanistic insights come from tissue cuts in embryonic mouse cerebellar slices (50). Radial tissue cuts into the EGL and underlying core result in wide gaps indicative of "circumferential" (tangential) tension in the EGL and PC layers. Horizontal cuts in the central core between EGL and ventricular zone result in wide gaps indicative of radial tension, likely involving RGCs and descending and ascending axons. These observations inspired a "multiphase wrinkling" model (50) that invokes 1) tangential expansion of the EGL driven by competition between radial and circumferential tension (perhaps generated in part by the meninges) and 2) folding mediated in part by differential radial tension related to the distribution of RGCs and BGCs. This model (137) has an elastic core surrounded by a fluid-like "film"; interactions between film-spanning and full-radius elastic fibers can account for why the outer film is relatively thick at the base of folds and relatively thin at the crowns (at least for the EGL). A proposed three-layer model (138) is based on differential stiffness of the ML, PC, and IGL; however, the ML is not yet present when folding is initiated. None of these models account for the accordion-like pattern of parallel cerebellar folds.

Here, I propose a cerebellar multilayer sandwich (CMS) model for cerebellar cortex that invokes additional features while sharing similarities with the above multiphase-wrinkling and three-layer models, the cerebral DES+ model, and my original cerebellar TBM model (1). The CMS model involves up to five layers, but fewer at early and late developmental stages, and includes five major tenets. Tenet 1, radially biased tension, generated early on mainly by BGC and RGC processes reaching the pial surface and later by PC dendrites and GC ascending axons reaching the ML, should keep cerebellar cortex thin and promote tangential expansion of the IGL, PC, ML, and EGL layers. Tenet 2, anisotropic tangential tension in the ML along parallel fibers, should promote folding along the parallel fiber axis (as in a package of spaghetti noodles) and thereby account for accordion-like cerebellar folding (1) and also elongation of the unfolded cerebellum in macaques and humans (127) along the higher-compliance axis (mainly antero-posterior) compared to the stiffer axis (mainly medio-lateral). Tenet 3, tangential tension in the meningeal layers, may come from stretching of the pial basal lamina and thick arachnoid layer. The transient EGL might also contribute if GCP leading processes are under tension as they migrate in quasi-random directions. Tenet 4, tethering tension in cerebellar input (CF and MF) and output (PC) axons, should keep cerebellar WM compact (Fig. 8*C*), leading to a thin, highly convoluted cerebellar cortex enshrouding thin WM blades. Tenet 5, transsulcal adhesion, would link opposing sulcal banks, initially by the thick but transient arachnoid (133) and later by ECM linking apposed basal laminae, promoting further invagination by a zipping mechanism akin to that proposed for neocortex. Importantly, the current cerebellar CMS model lacks a clear mechanism to account for ACs and the formation of primary fissures.

Testing the CMS Model. Several approaches proposed above for the cerebral DES+ model may be adaptable for testing the CMS model: 1) Use photoablation to test for anisotropic tension in parallel fibers; PC dendrites; BGC and RGC radial processes; GC ascending axons; and CF, MF, and PC axons. 2) Analyze cerebellar gyrification mutants (e.g., ref. 139) as model systems for mechanistic analyses. 3) Examine pial and arachnoid mechanical properties and adhesive interactions using in vitro methods,

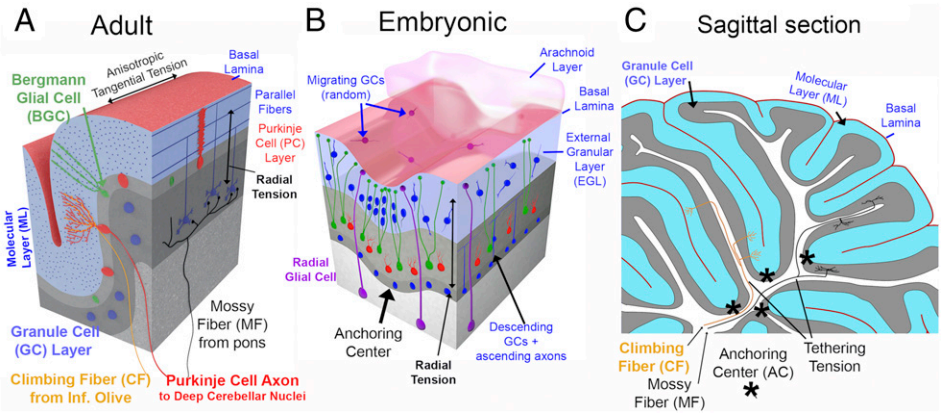

Fig. 8. Cerebellar circuits, development, and morphogenetic forces. (*A*) Adult cerebellar layers and input/output cell types (interneurons excluded). (*B*) Schematic of key developmental features at an early developmental stage (~E17.5 in mouse). (*C*) Adult mouse parasagittal section drawing, with putative tethering forces provided by input axons.

including organotypic cerebellar cultures (140). 4) Biomechanical measures: Does the ML layer show anisotropic compliance along vs. across the parallel fiber axis as predicted by the CMS model (*SI Appendix*, Topic 10)? 5) Critically evaluate computational models that incorporate biologically plausible tension patterns predicted by the CMS model.

Concluding Remarks

At a cellular level, mechanical tension is clearly involved in many key neurodevelopmental events in neurons and glial cells, typically involving cytoskeletal workhorse elements actomyosin and microtubules working against adhesion and pressure in a tensegrity framework. However, most biomechanical models of cellular developmental events remain piecemeal rather than comprehensive and qualitative rather than quantitative.

At a tissue level, the jury is still out regarding mechanisms of cerebral cortical expansion and folding. I contend that the DES+ cortical model has the greatest explanatory power among extant models. However, to incisively resolve ongoing controversies, it is vital that fresh approaches be brought to bear, such as the photoablation approach advocated herein, along with computational models that explicitly incorporate multiple types of tension. For subcortical nuclei, a simple quasi-isotropic tension model is highly plausible, but it has yet to be critically evaluated. For cerebellar cortex, the CMS model explains many key events but does not account for others such as the formation of anchoring centers. The general TBM model also provides attractive explanations for other distinctive CNS structures such as the retinal fovea and the hippocampal perforant pathway (*SI Appendix*, Topic 11). Broader exploration of what forces and cellular interactions drive morphogenesis in diverse organisms evolutionarily and diverse structures morphologically may reveal how a basic set of developmental mechanisms combines to generate the amazing diversity of CNS structures in the animal kingdom.

Countless studies in recent decades have implicated thousands of genes, macromolecules, and regulatory molecules in regulating various aspects of morphogenesis. All molecular interactions that affect the shape of a cell or tissue must pass through the biomechanical bottleneck of using forces, especially tension and pressure, to mediate morphogenetic change. A broad challenge for the future is to strive for stronger and deeper links across levels, so that specific morphogenetic events can be characterized not only by specifying the forces involved but also by explaining how these forces are dynamically regulated in living systems.

Data Availability. Neuroimaging data for *SI Appendix*, Fig. S2 have been deposited in the Brain Analysis Library of Spatial maps and Atlases (BALSA) database (https://balsa.wustl.edu/study/B432K).

ACKNOWLEDGMENTS. I thank Linda Richards, Phil Bayly, Henry Kennedy, John Cooper, Tim Coalson, Katie Long, Andrew Lawton, Alex Joyner, Colette Dehay, Ferechte Razavi, Joshua Sanes, Robert Hammond, Ken Knoblauch, and Wieland Huttner for insightful discussions and comments; the reviewers for constructive suggestions; and Mark Hallett and Matthew Glasser for technical contributions. This work was supported by NIH Grant MH060974-26. Human neuroimaging data for *SI Appendix*, Fig. S2 were provided by the Human Connectome Project, WU-Minn Consortium (principal investigators: D.C.V.E. and Kamil Ugurbil; Grant 1U54MH091657) funded by the 16 NIH Institutes and Centers that support the NIH Blueprint for Neuroscience Research, and by the McDonnell Center for Systems Neuroscience at Washington University.

1. D. C. Van Essen, A tension-based theory of morphogenesis and compact wiring in the central nervous system. *Nature* **385**, 313–318 (1997).
2. B. L. Finlay, R. B. Darlington, Linked regularities in the development and evolution of mammalian brains. *Science* **268**, 1578–1584 (1995).
3. D. C. Van Essen, "Cerebral cortical folding patterns in primates: Why they vary and what they signify" in *Evolution of Nervous Systems*, J. Kaas, Ed. (Academic Press, Oxford, UK, 2007), pp. 267–276.
4. B. Mota, S. Herculano-Houzel, BRAIN STRUCTURE. Cortical folding scales universally with surface area and thickness, not number of neurons. *Science* **349**, 74–77 (2015).
5. D. W. Thompson, *On Growth and Form* (Cambridge University Press, 1917).
6. T. J. Dennerll, H. C. Joshi, V. L. Steel, R. E. Buxbaum, S. R. Heidemann, Tension and compression in the cytoskeleton of PC-12 neurites. II: Quantitative measurements. *J. Cell Biol.* **107**, 665–674 (1988).
7. P. Lamoureux, R. E. Buxbaum, S. R. Heidemann, Direct evidence that growth cones pull. *Nature* **340**, 159–162 (1989).
8. D. Bray, Mechanical tension produced by nerve cells in tissue culture. *J. Cell Sci.* **37**, 391–410 (1979).
9. K. Franze, P. A. Janmey, J. Guck, Mechanics in neuronal development and repair. *Annu. Rev. Biomed. Eng.* **15**, 227–251 (2013).
10. E. Ruoslahti, Brain extracellular matrix. *Glycobiology* **6**, 489–492 (1996).
11. F. N. Soria *et al.*, Synucleinopathy alters nanoscale organization and diffusion in the brain extracellular space through hyaluronan remodeling. *Nat. Commun.* **11**, 3440 (2020).
12. P. Mastorakos, D. McGavern, The anatomy and immunology of vasculature in the central nervous system. *Sci. Immunol.* **4**, eaav0492 (2019).
13. A. I. Athamneh, D. M. Suter, Quantifying mechanical force in axonal growth and guidance. *Front. Cell. Neurosci.* **9**, 359 (2015).
14. N. C. Heer, A. C. Martin, Tension, contraction and tissue morphogenesis. *Development* **144**, 4249–4260 (2017).
15. J. Lantoine *et al.*, Matrix stiffness modulates formation and activity of neuronal networks of controlled architectures. *Biomaterials* **89**, 14–24 (2016).
16. B. Fuller, *Synergetics: Explorations in the Geometry of Thinking* (McMillan, 1982).
17. D. E. Ingber, N. Wang, D. Stamenovic, Tensegrity, cellular biophysics, and the mechanics of living systems. *Rep. Prog. Phys.* **77**, 046603 (2014).
18. M. E. Chicurel, C. S. Chen, D. E. Ingber, Cellular control lies in the balance of forces. *Curr. Opin. Cell Biol.* **10**, 232–239 (1998).
19. D. E. Ingber, Opposing views on tensegrity as a structural framework for understanding cell mechanics. *J. Appl. Physiol.* **89**, 1663–1670 (2000).
20. A. Goriely, *The Mathematics and Mechanics of Biological Growth* (Interdisciplinary Applied Mathematics, Springer, New York, NY, 2017).
21. J. Nie *et al.*, Axonal fiber terminations concentrate on gyri. *Cereb. Cortex* **22**, 2831–2839 (2012).
22. G. F. Striedter, S. Srinivasan, E. S. Monuki, Cortical folding: When, where, how, and why? *Annu. Rev. Neurosci.* **38**, 291–307 (2015).
23. H. G. B. Allen, *Background to Buckling* (McGraw-Hill Book Company Limited, London, England, 1980).
24. A. Fan, M. S. H. Joy, T. Saif, A connected cytoskeleton network generates axonal tension in embryonic Drosophila. *Lab Chip* **19**, 3133–3139 (2019).
25. A. P. Barnes, F. Polleux, Establishment of axon-dendrite polarity in developing neurons. *Annu. Rev. Neurosci.* **32**, 347–381 (2009).
26. T. D. Pollard, R. D. Goldman, Overview of the cytoskeleton from an evolutionary perspective. *Cold Spring Harb. Perspect. Biol.* **10**, a030288 (2018).
27. E. W. Dent, S. L. Gupton, F. B. Gertler, The growth cone cytoskeleton in axon outgrowth and guidance. *Cold Spring Harb. Perspect. Biol.* **3**, a001800 (2011).
28. Q. Xiao, X. Hu, Z. Wei, K. Y. Tam, Cytoskeleton molecular motors: Structures and their functions in neuron. *Int. J. Biol. Sci.* **12**, 1083–1092 (2016).
29. J. A. Hammer 3rd, W. Wagner, Functions of class V myosins in neurons. *J. Biol. Chem.* **288**, 28428–28434 (2013).
30. D. B. Arnold, G. Gallo, Structure meets function: Actin filaments and myosin motors in the axon. *J. Neurochem.* **129**, 213–220 (2014).
31. M. T. Kelliher, H. A. Saunders, J. Wildonger, Microtubule control of functional architecture in neurons. *Curr. Opin. Neurobiol.* **57**, 39–45 (2019).
32. L. C. Kapitein, C. C. Hoogenraad, Building the neuronal microtubule cytoskeleton. *Neuron* **87**, 492–506 (2015).
33. M. Schliwa, G. Woehlke, Molecular motors. *Nature* **422**, 759–765 (2003).
34. J. Z. Kechagia, J. Ivaska, P. Roca-Cusachs, Integrins as biomechanical sensors of the microenvironment. *Nat. Rev. Mol. Cell Biol.* **20**, 457–473 (2019).
35. A. F. Pegoraro, P. Janmey, D. A. Weitz, Mechanical properties of the cytoskeleton and cells. *Cold Spring Harb. Perspect. Biol.* **9**, a022038 (2017).
36. K. R. Long, W. B. Huttner, How the extracellular matrix shapes neural development. *Open Biol.* **9**, 180216 (2019).
37. A. Gato, M. E. Desmond, Why the embryo still matters: CSF and the neuroepithelium as interdependent regulators of embryonic brain growth, morphogenesis and histiogenesis. *Dev. Biol.* **327**, 263–272 (2009).
38. J. Faix, K. Rottner, The making of filopodia. *Curr. Opin. Cell Biol.* **18**, 18–25 (2006).
39. C. E. Chan, D. J. Odde, Traction dynamics of filopodia on compliant substrates. *Science* **322**, 1687–1691 (2008).
40. K. Hu, L. Ji, K. T. Applegate, G. Danuser, C. M. Waterman-Storer, Differential transmission of actin motion within focal adhesions. *Science* **315**, 111–115 (2007).
41. J. Rajagopalan, A. Tofangchi, M. T. A Saif, Drosophila neurons actively regulate axonal tension in vivo. *Biophys. J.* **99**, 3208–3215 (2010).
42. L. Soares, M. Parisi, N. M. Bonini, Axon injury and regeneration in the adult Drosophila. *Sci. Rep.* **4**, 6199 (2014).
43. B. G. Condron, K. Zinn, Regulated neurite tension as a mechanism for determination of neuronal arbor geometries in vivo. *Curr. Biol.* **7**, 813–816 (1997).
44. M. O'Toole, P. Lamoureux, K. E. Miller, Measurement of subcellular force generation in neurons. *Biophys. J.* **108**, 1027–1037 (2015).
45. K. Franze *et al.*, Neurite branch retraction is caused by a threshold-dependent mechanical impact. *Biophys. J.* **97**, 1883–1890 (2009).

46. B. J. Pfister, A. Iwata, D. F. Meaney, D. H. Smith, Extreme stretch growth of integrated axons. *J. Neurosci.* **24**, 7978–7983 (2004).
47. P. Lamoureux, S. R. Heidemann, N. R. Martzke, K. E. Miller, Growth and elongation within and along the axon. *Dev. Neurobiol.* **70**, 135–149 (2010).
48. W. Lu, M. Winding, M. Lakonishok, J. Wildonger, V. I. Gelfand, Microtubule-microtubule sliding by kinesin-1 is essential for normal cytoplasmic streaming in Drosophila oocytes. *Proc. Natl. Acad. Sci. U.S.A.* **113**, E4995–E5004 (2016).
49. U. Del Castillo, W. Lu, M. Winding, M. Lakonishok, V. I. Gelfand, Pavarotti/MKLP1 regulates microtubule sliding and neurite outgrowth in Drosophila neurons. *Curr. Biol.* **25**, 200–205 (2015).
50. A. K. Lawton *et al*., Cerebellar folding is initiated by mechanical constraints on a fluid-like layer without a cellular pre-pattern. *eLife* **8**, e45019 (2019).
51. Y. B. Lu *et al*., Viscoelastic properties of individual glial cells and neurons in the CNS. *Proc. Natl. Acad. Sci. U.S.A.* **103**, 17759–17764 (2006).
52. P. Crino *et al*., Presence and phosphorylation of transcription factors in developing dendrites. *Proc. Natl. Acad. Sci. U.S.A.* **95**, 2313–2318 (1998).
53. B. Han, R. Zhou, C. Xia, X. Zhuang, Structural organization of the actin-spectrin-based membrane skeleton in dendrites and soma of neurons. *Proc. Natl. Acad. Sci. U.S.A.* **114**, E6678–E6685 (2017).
54. J. A. Cooper, Cell biology in neuroscience: Mechanisms of cell migration in the nervous system. *J. Cell Biol.* **202**, 725–734 (2013).
55. T. Fujioka, N. Kaneko, K. Sawamoto, Blood vessels as a scaffold for neuronal migration. *Neurochem. Int.* **126**, 69–73 (2019).
56. E. Taverna, M. Götz, W. B. Huttner, The cell biology of neurogenesis: Toward an understanding of the development and evolution of the neocortex. *Annu. Rev. Cell Dev. Biol.* **30**, 465–502 (2014).
57. M. Penisson, J. Ladewig, R. Belvindrah, F. Francis, Genes and mechanisms involved in the generation and amplification of basal radial glial cells. *Front. Cell. Neurosci.* **13**, 381 (2019).
58. Y. Kosodo *et al*., Regulation of interkinetic nuclear migration by cell cycle-coupled active and passive mechanisms in the developing brain. *EMBO J.* **30**, 1690–1704 (2011).
59. B. E. Ostrem, J. H. Lui, C. C. Gertz, A. R. Kriegstein, Control of outer radial glial stem cell mitosis in the human brain. *Cell Rep.* **8**, 656–664 (2014).
60. K. E. Garcia, R. J. Okamoto, P. V. Bayly, L. A. Taber, Contraction and stress-dependent growth shape the forebrain of the early chicken embryo. *J. Mech. Behav. Biomed. Mater.* **65**, 383–397 (2017).
61. M. P. Lun, E. S. Monuki, M. K. Lehtinen, Development and functions of the choroid plexus-cerebrospinal fluid system. *Nat. Rev. Neurosci.* **16**, 445–457 (2015).
62. M. K. Lehtinen *et al*., The cerebrospinal fluid provides a proliferative niche for neural progenitor cells. *Neuron* **69**, 893–905 (2011).
63. S. A. Bayer, J. Altman, *The Human Brain During the Late First Trimester* (Atlas of Human Central Nervous System Development, CRC Press, 2006).
64. J. Mojsilović, N. Zecević, Early development of the human thalamus: Golgi and Nissl study. *Early Hum. Dev.* **27**, 119–144 (1991).
65. I. H. Smart, C. Dehay, P. Giroud, M. Berland, H. Kennedy, Unique morphological features of the proliferative zones and postmitotic compartments of the neural epithelium giving rise to striate and extrastriate cortex in the monkey. *Cereb. Cortex* **12**, 37–53 (2002).
66. P. Rakic, Neurons in rhesus monkey visual cortex: Systematic relation between time of origin and eventual disposition. *Science* **183**, 425–427 (1974).
67. C. Dehay, P. Giroud, M. Berland, I. Smart, H. Kennedy, Modulation of the cell cycle contributes to the parcellation of the primate visual cortex. *Nature* **366**, 464–466 (1993).
68. I. Kostović, G. Sedmak, M. Judaš, Neural histology and neurogenesis of the human fetal and infant brain. *Neuroimage* **188**, 743–773 (2019).
69. I. Bystron, C. Blakemore, P. Rakic, Development of the human cerebral cortex: Boulder committee revisited. *Nat. Rev. Neurosci.* **9**, 110–122 (2008).
70. A. J. Jiménez, M. D. Domínguez-Pinos, M. M. Guerra, P. Fernández-Llebrez, J. M. Pérez-Fígares, Structure and function of the ependymal barrier and diseases associated with ependyma disruption. *Tissue Barriers* **2**, e28426 (2014).
71. S. Whish *et al*., The inner CSF-brain barrier: Developmentally controlled access to the brain via intercellular junctions. *Front. Neurosci.* **9**, 16 (2015).
72. T. J. Nowakowski, A. A. Pollen, C. Sandoval-Espinosa, A. R. Kriegstein, Transformation of the radial glia scaffold demarcates two stages of human cerebral cortex development. *Neuron* **91**, 1219–1227 (2016).
73. P. Rakic, Developmental and evolutionary adaptations of cortical radial glia. *Cereb. Cortex* **13**, 541–549 (2003).
74. M. Betizeau *et al*., Precursor diversity and complexity of lineage relationships in the outer subventricular zone of the primate. *Neuron* **80**, 442–457 (2013).
75. C. Llinares-Benadero, V. Borrell, Deconstructing cortical folding: Genetic, cellular and mechanical determinants. *Nat. Rev. Neurosci.* **20**, 161–176 (2019).
76. I. Bystron, P. Rakic, Z. Molnár, C. Blakemore, The first neurons of the human cerebral cortex. *Nat. Neurosci.* **9**, 880–886 (2006).
77. K. Sekine, T. Honda, T. Kawauchi, K. Kubo, K. Nakajima, The outermost region of the developing cortical plate is crucial for both the switch of the radial migration mode and the Dab1-dependent "inside-out" lamination in the neocortex. *J. Neurosci.* **31**, 9426–9439 (2011).
78. C. C. Gertz, A. R. Kriegstein, Neuronal migration dynamics in the developing ferret cortex. *J. Neurosci.* **35**, 14307–14315 (2015).
79. B. G. Rash *et al*., Gliogenesis in the outer subventricular zone promotes enlargement and gyrification of the primate cerebrum. *Proc. Natl. Acad. Sci. U.S.A.* **116**, 7089–7094 (2019).
80. J. Candiello *et al*., Biomechanical properties of native basement membranes. *FEBS J.* **274**, 2897–2908 (2007).
81. M. Marin-Padilla, The human brain intracerebral microvascular system: development and structure. *Front. Neuroanat.* **6**, 10.3389/fnana.2012.00038 (2012).
82. S. A. Bayer, J. Altman, *The Human Brain During the Second Trimester* (Atlas of Human Central Nervous System Development, CRC Press, 2005).
83. A. Duque, Z. Krsnik, I. Kostović, P. Rakic, Secondary expansion of the transient subplate zone in the developing cerebrum of human and nonhuman primates. *Proc. Natl. Acad. Sci. U.S.A.* **113**, 9892–9897 (2016).
84. H. J. Luhmann, S. Kirischuk, W. Kilb, The superior function of the subplate in early neocortical development. *Front. Neuroanat.* **12**, 97 (2018).
85. A. Hoerder-Suabedissen, Z. Molnár, Morphology of mouse subplate cells with identified projection targets changes with age. *J. Comp. Neurol.* **520**, 174–185 (2012).
86. K. L. Allendoerfer, C. J. Shatz, The subplate, a transient neocortical structure: Its role in the development of connections between thalamus and cortex. *Annu. Rev. Neurosci.* **17**, 185–218 (1994).
87. A. Batardière *et al*., Early specification of the hierarchical organization of visual cortical areas in the macaque monkey. *Cereb. Cortex* **12**, 453–465 (2002).
88. S. M. Catalano, R. T. Robertson, H. P. Killackey, Early ingrowth of thalamocortical afferents to the neocortex of the prenatal rat. *Proc. Natl. Acad. Sci. U.S.A.* **88**, 2999–3003 (1991).
89. I. Žunić Išasegi *et al*., Interactive histogenesis of axonal strata and proliferative zones in the human fetal cerebral wall. *Brain Struct. Funct.* **223**, 3919–3943 (2018).
90. T. A. Coogan, D. C. Van Essen, Development of connections within and between areas V1 and V2 of macaque monkeys. *J. Comp. Neurol.* **372**, 327–342 (1996).
91. X. Wang, D. R. Pettersson, C. Studholme, C. D. Kroenke, Characterization of laminar zones in the mid-gestation primate brain with magnetic resonance imaging and histological methods. *Front. Neuroanat.* **9**, 147 (2015).
92. X. Wang *et al*., Folding, but not surface area expansion, is associated with cellular morphological maturation in the fetal cerebral cortex. *J. Neurosci.* **37**, 1971–1983 (2017).
93. Z. Liu *et al*., Anatomical and diffusion MRI brain atlases of the fetal rhesus macaque brain at 85, 110 and 135 days gestation. *Neuroimage* **206**, 116310 (2020).
94. N. T. Markov *et al*., A weighted and directed interareal connectivity matrix for macaque cerebral cortex. *Cereb. Cortex* **24**, 17–36 (2014).
95. E. González-Arnay, M. González-Gómez, G. Meyer, A radial glia fascicle leads principal neurons from the pallial-subpallial boundary into the developing human insula. *Front. Neuroanat.* **11**, 111 (2017).
96. T. Tallinen *et al*., On the growth and form of cortical convolutions. *Nat. Phys.* **12**, 588–593 (2016).
97. K. R. Long *et al*., Extracellular matrix components HAPLN1, lumican, and collagen I cause hyaluronic acid-dependent folding of the developing human neocortex. *Neuron* **99**, 702–719.e6 (2018).
98. C. C. Hilgetag, H. Barbas, Role of mechanical factors in the morphology of the primate cerebral cortex. *PLoS Comput. Biol.* **2**, e22 (2006).
99. D. C. Van Essen *et al*., Cerebral cortical folding, parcellation, and connectivity in humans, nonhuman primates, and mice. *Proc. Natl. Acad. Sci. U.S.A.* **116**, 26173–26180 (2019).
100. M. Ono, K. S. Kubik, C. D. Abernathey, *Atlas of the Cerebral Sulci* (Thieme Medical Publishers, Inc., New York, NY, 1990).
101. W. Welker, "Why does cerebral cortex fissure and fold?" in *Cerebral Cortex*, E. G. Jones, A. Peters, Eds. (Springer, 1990), vol. P, pp. 3–136.
102. I. H. Smart, G. M. McSherry, Gyrus formation in the cerebral cortex of the ferret. II. Description of the internal histological changes. *J. Anat.* **147**, 27–43 (1986).
103. I. Ferrer, I. Fabregues, E. Condom, A Golgi study of the sixth layer of the cerebral cortex. II. The gyrencephalic brain of Carnivora, Artiodactyla and primates. *J. Anat.* **146**, 87–104 (1986).
104. D. P. Keeley, D. R. Sherwood, Tissue linkage through adjoining basement membranes: The long and the short term of it. *Matrix Biol.* **75–76**, 58–71 (2019).
105. M. F. Glasser *et al*., A multi-modal parcellation of human cerebral cortex. *Nature* **536**, 171–178 (2016).
106. C. D. Kroenke, P. V. Bayly, How forces fold the cerebral cortex. *J. Neurosci.* **38**, 767–775 (2018).
107. M. Ercsey-Ravasz *et al*., A predictive network model of cerebral cortical connectivity based on a distance rule. *Neuron* **80**, 184–197 (2013).
108. C. M. Owen, A. Howard, D. K. Binder, Hippocampus minor, calcar avis, and the Huxley-Owen debate. *Neurosurgery* **65**, 1098–1104, discussion 1104–1105 (2009).
109. V. Borrell, How cells fold the cerebral cortex. *J. Neurosci.* **38**, 776–783 (2018).
110. I. Reillo, C. de Juan Romero, M. Á. García-Cabezas, V. Borrell, A role for intermediate radial glia in the tangential expansion of the mammalian cerebral cortex. *Cereb. Cortex* **21**, 1674–1694 (2011).
111. M. Holland, S. Budday, A. Goriely, E. Kuhl, Symmetry breaking in wrinkling patterns: Gyri are universally thicker than sulci. *Phys. Rev. Lett.* **121**, 228002 (2018).
112. G. Xu, P. V. Bayly, L. A. Taber, Residual stress in the adult mouse brain. *Biomech. Model. Mechanobiol.* **8**, 253–262 (2009).
113. G. Xu *et al*., Axons pull on the brain, but tension does not drive cortical folding. *J. Biomech. Eng.* **132**, 071013 (2010).
114. L. Siklós, U. Kuhnt, A. Párducz, P. Szerdahelyi, Intracellular calcium redistribution accompanies changes in total tissue Na+, K+ and water during the first two hours of in vitro incubation of hippocampal slices. *Neuroscience* **79**, 1013–1022 (1997).
115. D. G. MacGregor, M. Chesler, M. E. Rice, HEPES prevents edema in rat brain slices. *Neurosci. Lett.* **303**, 141–144 (2001).
116. V. Borrell, I. Reillo, Emerging roles of neural stem cells in cerebral cortex development and evolution. *Dev. Neurobiol.* **72**, 955–971 (2012).

117. A. Kriegstein, S. Noctor, V. Martínez-Cerdeño, Patterns of neural stem and progenitor cell division may underlie evolutionary cortical expansion. *Nat. Rev. Neurosci.* **7**, 883–890 (2006).
118. D. P. Richman, R. M. Stewart, J. W. Hutchinson, V. S. Caviness Jr, Mechanical model of brain convolutional development. *Science* **189**, 18–21 (1975).
119. M. F. Yanik *et al*., Neurosurgery: Functional regeneration after laser axotomy. *Nature* **432**, 822 (2004).
120. X. C. Ju *et al*., The hominoid-specific gene TBC1D3 promotes generation of basal neural progenitors and induces cortical folding in mice. *eLife* **5**, e18197 (2016).
121. M. Florio *et al*., Human-specific gene ARHGAP11B promotes basal progenitor amplification and neocortex expansion. *Science* **347**, 1465–1470 (2015).
122. Y. Li *et al*., Induction of expansion and folding in human cerebral organoids. *Cell Stem Cell* **20**, 385–396.e3 (2017).
123. E. Karzbrun, A. Kshirsagar, S. R. Cohen, J. H. Hanna, O. Reiner, Human brain organoids on a chip reveal the physics of folding. *Nat. Phys.* **14**, 515–522 (2018).
124. D. C. Van Essen *et al*., Symmetry of cortical folding abnormalities in Williams syndrome revealed by surface-based analyses. *J. Neurosci.* **26**, 5470–5483 (2006).
125. C. W. Nordahl *et al*., Cortical folding abnormalities in autism revealed by surface-based morphometry. *J. Neurosci.* **27**, 11725–11735 (2007).
126. M. G. Norman, J. R. O'Kusky, The growth and development of microvasculature in human cerebral cortex. *J. Neuropathol. Exp. Neurol.* **45**, 222–232 (1986).
127. D. C. Van Essen, Surface-based atlases of cerebellar cortex in the human, macaque, and mouse. *Ann. N. Y. Acad. Sci.* **978**, 468–479 (2002).
128. R. V. Sillitoe, A. L. Joyner, Morphology, molecular codes, and circuitry produce the three-dimensional complexity of the cerebellum. *Annu. Rev. Cell Dev. Biol.* **23**, 549–577 (2007).
129. O. J. Larsell, *The Comparative Anatomy and Histology of the Cerebellum* (University of Minnesota Press, 1970).
130. Y. Shinoda, I. Sugihara, H. S. Wu, Y. Sugiuchi, The entire trajectory of single climbing and mossy fibers in the cerebellar nuclei and cortex. *Prog. Brain Res.* **124**, 173–186 (2000).
131. A. W. Leung, J. Y. H. Li, The molecular pathway regulating Bergmann glia and folia generation in the cerebellum. *Cerebellum* **17**, 42–48 (2018).
132. H. Komuro, E. Yacubova, E. Yacubova, P. Rakic, Mode and tempo of tangential cell migration in the cerebellar external granular layer. *J. Neurosci.* **21**, 527–540 (2001).
133. P. Haldipur *et al*., Spatiotemporal expansion of primary progenitor zones in the developing human cerebellum. *Science* **366**, 454–460 (2019).
134. C. I. De Zeeuw, T. M. Hoogland, Reappraisal of Bergmann glial cells as modulators of cerebellar circuit function. *Front. Cell. Neurosci.* **9**, 246 (2015).
135. A. Buffo, F. Rossi, Origin, lineage and function of cerebellar glia. *Prog. Neurobiol.* **109**, 42–63 (2013).
136. A. Sudarov, A. L. Joyner, Cerebellum morphogenesis: The foliation pattern is orchestrated by multi-cellular anchoring centers. *Neural Dev.* **2**, 26 (2007).
137. T. A. Engstrom, T. Zhang, A. K. Lawton, A. L. Joyner, J. M. Schwarz, Buckling without bending: A new paradigm in morphogenesis. *Phys. Rev. X* **8**, 041053 (2018).
138. E. Lejeune, A. Javili, J. Weickenmeier, E. Kuhl, C. Linder, Tri-layer wrinkling as a mechanism for anchoring center initiation in the developing cerebellum. *Soft Matter* **12**, 5613–5620 (2016).
139. K. Li, A. W. Leung, Q. Guo, W. Yang, J. Y. Li, Shp2-dependent ERK signaling is essential for induction of Bergmann glia and foliation of the cerebellum. *J. Neurosci.* **34**, 922–931 (2014).
140. F. Doussau *et al*., Organotypic cultures of cerebellar slices as a model to investigate demyelinating disorders. *Expert Opin. Drug Discov.* **12**, 1011–1022 (2017).